Full Text View

Volume 29, Issue 2 (February 1999)

**Journal of Physical Oceanography**
Article: pp. 231–239 | Abstract | PDF (157K)

# Gravity and Shear Wave Contributions to Nearshore Infragravity Motions

**T. C. Lippmann**

*Center for Coastal Studies, Scripps Institution of Oceanography, La Jolla, California*

**T. H. C. Herbers and E. B. Thornton**

*Department of Oceanography, Naval Postgraduate School, Monterey, California*

(Manuscript received May 12, 1997, in final form March 30, 1998)

DOI: 10.1175/1520-0485(1999)029<0231:GASWCT>2.0.CO;2

ABSTRACT

Data from a cross-shore array of nine collocated pressure sensors and bidirectional current meters, extending from the shoreline to approximately 4.5-m depth, are used to estimate the relative contributions of gravity waves (e.g., edge and leaky waves) and instabilities of the alongshore current (shear waves) to motions in the infragravity (frequencies nominally 0.004–0.05 Hz) band. The ratio between frequency-integrated velocity and pressure variances is shown to be approximately equal to $g/h$ for a broad spectrum of gravity waves independent of the mode mix of edge and leaky waves. Since shear waves have velocity to pressure variance ratios $\gg g/h$, this ratio can be used to estimate the relative contributions of gravity and shear waves to the infragravity band. Outside the surf zone where the shear in the alongshore current is relatively weak, the observed velocity to pressure variance ratios are approximately equal to $g/h$, consistent with a gravity-dominated wave field. Inside the surf zone where alongshore currents are strongly sheared, these ratios are up to a factor of 4 larger, indicating that shear waves contribute as much as 75% of the velocity variance in the infragravity band. Observed shear-wave-dominated infragravity band motions are confined to a narrow region of strong shear on the seaward side of the alongshore current maximum, and their cross-shore structure appears to be insensitive to changes in the beach profile, qualitatively consistent with theoretical predictions by linear stability analysis.





## 1. Introduction

Wave motions with periods of several minutes, longer than the periods of sea and

swell waves, were first observed in the nearshore by Munk (1949) who coined the name "surf beat." Subsequently they have been called infragravity waves to distinguish them from incident wind-generated gravity waves. Since Munk's initial observations, considerable effort has been focused on understanding the generation process and variability of infragravity waves and their importance to nearshore morphology. Extensive observations on natural beaches have shown that infragravity waves often dominate the spectra of inner surf zone and swash motions (e.g., Huntley 1976; Huntley et al. 1981; Holman 1981; Thornton and Guza 1982; Holman and Sallenger 1985;Sallenger and Holman 1987; and many others), particularly during storms when incident wave heights in shallow water are severely limited by breaking (e.g., Thornton and Guza 1982). The field data also indicate that infragravity motions are a complicated mixture of edge waves, obliquely propagating gravity waves trapped close to shore by multiple reflections from the shoreline and offshore refraction, and leaky waves, nearly shore-normal propagating gravity waves, which upon reflection from shore radiate to deep water or are dissipated on the continental shelf (Suhayda 1974; Bowen and Guza 1978; Huntley et al. 1981; Guza and Thornton 1985; Oltman-Shay and Guza 1987; Herbers et al. 1995a,b; and others).

In the shallow water approximation on a plane beach, the edge wave dispersion relation is given by

$$\sigma^2 = g|k_y|(2n + 1)\tan\beta \qquad n = 0, 1, 2, \ldots, \qquad (1)$$

where $\sigma$ and $k_y$ are the radian frequency and alongshore wavenumber respectively, $g$ is gravity, $n$ is the edge wave mode number, and $\beta$ is the beach slope (Eckart 1951). Observations of $\sigma$–$k_y$ spectra confirm the existence of strong resonances in the surf zone with typically a concentration of energy on edge wave dispersion curves (1) for low mode numbers (Huntley et al. 1981;Oltman-Shay and Guza 1987; Howd et al. 1991; and others). Leaky gravity waves occupy a continuum of smaller alongshore wavenumbers in the range

$$-\frac{\sigma^2}{g} < k_y < \frac{\sigma^2}{g}. \qquad (2)$$

Remotely generated leaky waves arriving from the open ocean may also contribute significantly to nearshore infragravity motions when local forcing is weak (Herbers et al. 1995a,b). In addition to edge and leaky waves, forced gravity waves may be present with any wavenumber.

Recent observations have shown that in addition to gravity (edge and leaky) waves, instabilities of the alongshore current, commonly referred to in the literature as shear waves (Bowen and Holman 1989; Oltman-Shay et al. 1989; Dodd and Thornton 1990; Howd et al. 1991; Dodd et al. 1992; and others), contribute significantly to surf zone motions at infragravity frequencies. Shear waves have alongshore phase speeds

$$\frac{\sigma}{|k_y|} \approx \overline{V}, \qquad (3)$$

where $\overline{V}$ is the mean alongshore current, that are typically much smaller than the phase speeds of the slowest [mode 0, Eq. (1)] gravity waves. Hence, shear waves are easily distinguished from edge and leaky gravity waves in $\sigma$–$k_y$ space (Bowen and Holman 1989; Oltman-Shay et al. 1989; Howd et al. 1991).

The different infragravity motions have been resolved qualitatively in field data with sparse alongshore arrays of spatially lagged current meters and sophisticated estimation techniques that optimally use the array cross-spectra to infer the frequency–alongshore wavenumber spectrum, $E(\sigma, k_y)$ (e.g., Oltman-Shay et al. 1989; Howd et al. 1992). Estimates of $E(\sigma, k_y)$ in the surf zone indicate that gravity and shear wave contributions to the infragravity band are roughly comparable (Howd et al. 1992).

The cross-shore variability of shear waves is difficult to quantify in field data owing to the complex cross-shore variations in standing gravity waves. Whereas progressive gravity waves with equi-partitioned kinetic and potential energy are distinguished easily from shear waves whose energy is nearly entirely kinetic (Bowen and Holman 1989), in standing gravity waves the energy partitioning varies with cross-shore position between entirely potential (at antinodes) and kinetic (at nodes). Hence, alongshore array measurements at a single cross-shore position may not be representative of the shear and gravity wave mix. In this paper the total energy of a broad gravity wave spectrum containing edge and leaky waves is shown to be approximately equi-partitioned between kinetic and potential energy, independent of the detailed mode mix. Thus, the ratio between velocity and pressure variances integrated over the infragravity band can be used to estimate the relative contributions of gravity and shear waves. The variance partitioning analysis technique is applied to field measurements from a cross-shore array of collocated pressure sensors and bidirectional current meters spanning the surf zone of a barred sandy beach.

## 2. Theory

### *a. Edge waves*

In the linear shallow water approximation a beach with straight and parallel depth contours ($h = h(x)$) supports edge wave solutions of the general form (Eckart 1951)

$$\Phi_n(x,\ y,\ t) = \frac{a_n g}{\sigma}\phi_n(k_y x)\ \sin(k_y y - \sigma t), \qquad (4)$$

where $\Phi$ is the velocity potential, $x$ and $y$ are the cross-shore and alongshore coordinates, $t$ is time, $n$ is the discrete edge-wave mode number, and $a_n$ is the modal amplitude at the shoreline. An eigenvalue problem for the cross-shore dependence function $\phi_n$ follows from vertically integrating the equations of motion, subject to the condition of no flow through the bottom and linear surface boundary conditions (e.g., Holman and Bowen 1979)

$$\frac{\partial}{\partial x}\left(gh\frac{\partial \phi_n}{\partial x}\right) + (\sigma^2 - gk_y^2 h)\phi_n = 0. \qquad (5)$$

On a plane beach with slope $\beta$, (5) yields solutions of the form (Eckart 1951)

$$\phi_n(k_y x) = L_n(2|k_y x|)e^{-|k_y x|}, \qquad (6)$$

where $L_n$ is the Laguerre polynomial of order $n$, and the corresponding eigenvalues are given by the dispersion relation (1).

For a continuous spectrum of edge waves the velocity potential can be expressed as

$$\Phi_n(x,\ y,\ t) = \int_{-\infty}^{\infty} dZ_n(k_y)\frac{g}{i\sigma}\phi_n(k_y x)e^{i(k_y y - \sigma t)} + *, \qquad (7)$$

where the asterisk indicates the complex conjugate and $dZ_n$ is the complex shoreline amplitude function with a density spectrum

$$E_n(k_y)dk_y = 2\mathbf{E}\{dZ_n(k_y)dZ^*_n(k_y)\}, \qquad (8)$$

with $\mathbf{E}\{\ \}$ denoting the expected value. The corresponding surface elevations $\eta_n$ (or pressure head $p_n$) and velocity components $u_n$ (cross shore) and $v_n$ (alongshore) are given by

$$\begin{aligned}
\eta_n = p_n &= -\frac{1}{g}\frac{\partial \Phi_n}{\partial t} \\
&= \int_{-\infty}^{\infty} dZ_n(k_y)\phi_n(k_y x)e^{i(k_y y - \sigma t)} + * \\
u_n = \frac{\partial \Phi_n}{\partial x} &= \int_{-\infty}^{\infty} dZ_n(k_y)\frac{g}{i\sigma}\frac{\partial \phi_n(k_y x)}{\partial x}e^{i(k_y y - \sigma t)} + * \\
v_n = \frac{\partial \Phi_n}{\partial y} &= \int_{-\infty}^{\infty} dZ_n(k_y)\frac{gk_y}{\sigma}\phi_n(k_y x)e^{i(k_y y - \sigma t)} + * \qquad (9)
\end{aligned}$$

with wavenumber spectra

$$E_{\eta,n}(k_y;\, x) = \phi_n^2(k_y x) E_n(k_y)$$

$$E_{u,n}(k_y;\, x) = \left(\frac{g}{\sigma}\frac{\partial \phi_n(k_y x)}{\partial x}\right)^2 E_n(k_y)$$

$$E_{v,n}(k_y;\, x) = \left(\frac{g k_y}{\sigma}\phi_n(k_y x)\right)^2 E_n(k_y). \qquad (10)$$

Field observations of alongshore wavenumber spectra (e.g., Oltman-Shay and Guza 1987) indicate that the energy of edge wave modes is fairly evenly distributed over a range of wavenumbers, possibly because the nonlinear forcing of edge waves by incident wind waves is a broadband process (e.g., Bowen and Guza 1978; Herbers et al. 1995b). For simplicity we assume that for a given mode $n$ the edge wave variance is distributed uniformly in wavenumber space, that is, the wavenumber density spectrum $E_n(k_y) = E_n$. The pressure and velocity variances can be evaluated at any location $x$ by substituting (6) in (10) and integrating over all possible wavenumbers [using the dispersion relation Eq. (1)]:

$$\langle p_n^2 \rangle = E_n \int_{-\infty}^{\infty} \phi_n^2 \, dk_y = E_n\left(\frac{\tan\beta}{h}\right)$$

$$\langle u_n^2 \rangle = E_n \int_{-\infty}^{\infty} \left(\frac{g}{\sigma}\frac{\partial \phi_n}{\partial x}\right)^2 dk_y = E_n\left(\frac{g\,\tan\beta}{2h^2}\right)$$

$$\langle v_n^2 \rangle = E_n \int_{-\infty}^{\infty} \left(\frac{g k_y}{\sigma}\phi_n\right)^2 dk_y = E_n\left(\frac{g\,\tan\beta}{2h^2}\right). \qquad (11)$$

Although the integration limits are $(-\infty, \infty)$, $\Phi_n$ is small for large values of $|k_y|$ [the exponential term in Eq. (6)]. Hence, short wavelength edge waves that are trapped shoreward of the instrument location $x$ do not contribute to the integrals. The integrated edge wave variances decay away from the shoreline as simple functions of the depth, with pressures (velocities) proportional to $h^{-1}$ ($h^{-2}$). Herbers et al. (1995a) derived the same depth dependence for a directionally isotropic gravity wave field in slowly varying depth. Whereas the present results, obtained from exact shallow water edge wave solutions, are valid only on a plane beach, the asymptotic WKB results of Herbers et al. are valid on arbitrary (monotonic sloping) beach profiles, but only far from shore beyond the trapping point of low mode edge waves. Ratios of velocity to pressure variances are given by

$$\frac{\langle u_n^2 \rangle}{\langle p_n^2 \rangle} = \frac{\langle v_n^2 \rangle}{\langle p_n^2 \rangle} = \frac{g}{2h}. \qquad (12)$$

Note that the simple relations (11), (12) are independent of the edge-wave mode number.

### *b. Leaky waves*

As the edge-wave mode number $n$ increases, the range of possible frequencies that contribute to measurements at a location $x$ increases [i.e., the exponential tail of Eq. (6) for $|k_y x| \gg 1$ shifts to larger values of $\sigma$; Eq. (1)]. Hence, the assumption of a uniform spectrum is not realistic for high mode edge waves. Additionally, the shallow water approximation used here is inaccurate for high mode edge waves and breaks down for wave components with small alongshore wavenumbers [leaky waves, Eq. (2)] that extend to deep water. A different approximation is needed to describe the cross-shore variability of pressure and velocity variances of leaky waves and high mode edge waves. Close to shore (where $v \ll u$) the cross-shore dependence functions $\Phi$ of leaky waves and high mode edge waves are indistinguishable and are described accurately (away from the immediate vicinity of the shoreline) by a shallow water WKB approximation [cf. Eq. (6) in Guza and Thornton (1985) and Eq. (A8) in Herbers et al. (1995a)]. In broad spectra, the standing wave nodal structure can be neglected, and pressure and velocity variances are given by the standard shoaling relations

$$\langle p_{\mathrm{lw}}^2 \rangle = \frac{E}{\sigma}\left(\frac{g}{h}\right)^{1/2}$$

$$\langle u_{\mathrm{lw}}^2 \rangle = \frac{E}{\sigma}\left(\frac{g}{h}\right)^{3/2}$$

$$\langle v_{\mathrm{lw}}^2 \rangle = 0, \qquad (13)$$

with $E$ an arbitrary energy constant. Thus, close to shore, the pressure (velocity) variances of leaky waves (and high mode edge waves) have depth dependencies of $h^{-1/2}$ ($h^{-3/2}$) that are weaker than the $h^{-1}$ ($h^{-2}$) dependencies of low mode edge wave variances. Ratios of leaky wave velocity and pressure variances are given by

$$\frac{\langle u_{\mathrm{lw}}^2 \rangle}{\langle p_{\mathrm{lw}}^2 \rangle} = \frac{g}{h}$$

$$\frac{\langle v_{\mathrm{lw}}^2 \rangle}{\langle p_{\mathrm{lw}}^2 \rangle} = 0. \qquad (14)$$

### *c. Shear waves*

Bowen and Holman (1989) examined the stability of a steady alongshore current $\overline{V}(x)$ to small perturbations using a linear vorticity equation based on the shallow water equations and the rigid-lid approximation. They showed that in the region of strong seaward shear ($d|\overline{V}|/dx < 0$), instabilities develop in the form of alongshore propagating velocity oscillations (shear waves). Ratios between variances of shear wave velocities and associated pressure fluctuations scale roughly as (Bowen and Holman 1989)

$$\frac{\langle u_{\mathrm{sh}}^2 \rangle}{\langle p_{\mathrm{sh}}^2 \rangle}, \frac{\langle v_{\mathrm{sh}}^2 \rangle}{\langle p_{\mathrm{sh}}^2 \rangle} = O\left(\frac{g^2}{\overline{V}^2}\right). \qquad (15)$$

### *d. Total velocity to pressure variance ratio*

Whereas the velocity to pressure variance ratios of the individual $u$ and $v$ components of gravity waves are sensitive to the edge–leaky wave mode mix [Eqs. (12) and (14)], the normalized ratio of total velocity to pressure variance $R$,

$$R = \frac{\langle u^2 \rangle + \langle v^2 \rangle}{\langle p^2 \rangle} \Big/ \frac{g}{h}, \qquad (16)$$

is 1 (i.e., equi-partitioning of kinetic and potential energy) independent of the mode mix. For shear waves [Eq. (15)], $R = O(gh/\overline{V}^2)$, that is, $\gg 1$ for natural alongshore currents with typically small Froude numbers (e.g., Oltman-Shay et al. 1989). Hence, (16) can be used to estimate the contributions of gravity waves and shear waves to the infragravity band. If the gravity and shear wave velocity fluctuations are assumed to be statistically independent, then the fraction $\alpha$ of the infragravity velocity variance contributed by shear waves is approximately given by

$$\alpha = 1 - 1/R. \qquad (17)$$

## 3. Numerical calculations

Kirby et al. (1981) and Howd et al. (1992) show that nonplanar bathymetry and alongshore currents found on natural beaches can change significantly the cross-shore structure of individual edge wave modes. Thus, the theoretical velocity to pressure variance ratios for a plane beach may not be accurate on nonplanar topographies or in the presence of an alongshore current. Here, we use the numerical methods of Holman and Bowen (1979) and Howd et al. (1992) to obtain solutions of the shallow water edge wave equation [e.g., Eq. (6)] for realistic bottom and longshore current profiles. Howd

et al. verified the accuracy of numerically predicted dispersion relations (within ±0.1% in $k_y$) through comparisons with known analytical solutions for plane and exponential beaches, as well as Kenyon's (1972) approximation for edge waves on weak currents.

Velocity and pressure variances were computed for an ensemble of edge wave modes 0–16 on beach profiles representative of the field data (described below). The edge wave variance at the shoreline was distributed uniformly over the infragravity frequency range 0.004–0.05 Hz, and between individual modes. The beach profile is approximated by the general form

$$h = x\tan\beta_2 + \frac{a_1}{\tan\beta_1}(\tan\beta_1 - \tan\beta_2)\tanh\left(\frac{x\tan\beta_1}{a_1}\right) - a_2\exp\left[-5\left(\frac{x - x_c}{x_c}\right)^2\right], \quad (18)$$

where $\tan\beta_1$ is the foreshore slope, $\tan\beta_2$ is the offshore slope, $x_c$ is the location of the bar crest, and the coefficients $a_1$ and $a_2$ are determined by fitting the profile to the measured bathymetry. For a plane beach of constant slope, $\tan\beta_2 = \tan\beta_1$, and for a nonbarred beach, $a_2 = 0$ (Putrevu and Svendsen 1992). The synthetic barred profile ($\tan\beta_1 = 0.070$, $\tan\beta_2 = 0.0064$, $a_1 = 2.93$, $a_2 = 1.60$, $x_c = 92$ m) that provides a good fit to the profile surveyed on 11 October 1990 during the Delilah experiment is shown in Fig. 1 (lower panel).

The numerically predicted velocity to pressure variance ratios for a concave beach profile with and without a bar are within ±15% of the value 1 for a plane beach (Fig. 1). Computations incorporating realistic alongshore current profiles (not shown; see Howd et al. 1992), with equal contributions of up- and downcoast traveling edge waves yield velocity to pressure variance ratios that are within a few percent of the predicted values without an alongshore current. Although the cross-shore structure (i.e., locations of nodes and antinodes) of monochromatic edge waves is strongly affected by variations in depth and mean flow, bulk properties of a broad spectrum of edge waves are insensitive to the detailed bathymetry and the presence of currents, and are well described by the analytical results.

## 4. Field data

The field data examined in this study were obtained on a sandy, barred ocean beach during the Delilah experiment, held at the Army Corps of Engineers Field Research Facility in Duck, North Carolina, in the fall of 1990. For details of the experiment see Birkemeier (1991) and Thornton and Kim (1993). Bidirectional velocity and near-bottom pressure measurements were collected at nine locations along a cross-shore transect that spans the surf zone (Fig. 2). The instruments were sampled continuously at 8 Hz.

The beach at Duck runs approximately north–south and faces the Atlantic Ocean on the U.S. central eastern seaboard. Offshore bottom contours are nearly straight and parallel with a mean offshore slope of 0.0064. During Delilah, there was a single, persistent alongshore bar in the surf zone approximately 80 m offshore. On 11 and 12 October the bar was linear, with a bar–trough relief of about 0.5 m over 50 m. An example bathymetry map from 12 October is shown in Fig. 3. The cross-shore bottom profile along the instrumented transect is shown in Fig. 2.

The present analysis is focused on an 11-day period from 6 to 16 October, with offshore significant wave heights ranging from 0.4 to 2.5 m. A summary of wave, current, and wind conditions during Delilah can be found in Thornton and Kim (1993).

## 5. Results

Infragravity velocity and pressure variances were estimated from 34.1-min data records by integrating the spectra over the frequency range 0.004–0.05 Hz. The evolution of root-mean-square (rms) fluctuations over the duration of the experiment from a sensor located about 70 m offshore is shown in Fig. 4. Observations at other instruments inside the surf zone are generally similar. Two extratropical storms passed during the experiment (on 9 and 13 October) radiating long-crested swell from the southeast (between 40° and 20° clockwise from shore normal). Alongshore currents driven by these swells were predominantly toward the north. A weak northeaster (on 16 October) generated higher-frequency waves approaching the coast from the northeast (about 20° counterclockwise from shore normal) that caused a brief reversal of the alongshore current toward the south. The observed normalized velocity to pressure variance ratios $R$ at each sensor

position are shown in Fig. 5. Examples of the cross-shore variation of $R$ in relation to the beach and alongshore current profiles are shown in Figs. 6–8.

Early in the experiment (prior to 10 October) the beach profile was terracelike (Fig. 2). The mean alongshore currents were strongly tidally modulated at any particular cross-shore position within the surf zone. Thornton and Kim (1993) show that the alongshore current maximum moves on and offshore in response to the tidal variations in breaking patterns relative to the shoreline and the sand bar. Although offshore wave heights do not change significantly during the early part of the experiment, breaking wave heights in a saturated surf zone are depth-limited and thus increase in response to a tide-induced increase in sea level. Hence wave heights in the surf zone vary in phase with the tide. Thornton and Kim show that the associated changes in radiation stress gradients cause a similar tidal modulation of the mean alongshore current $\overline{V}$ with the local $\overline{V}$ and rms wave height in-phase shoreward of the $\overline{V}$ maximum and 180° out of phase seaward of the $\overline{V}$ maximum. Whereas rms infragravity velocities inside the surf zone also show substantial tidal variations (e.g., Fig. 4), rms infragravity pressures are not strongly tidally modulated, except very near the shoreline (not shown). The similarity of tidal modulations of $\overline{V}$ and infragravity velocities that are absent in the infragravity pressure signal suggest that shear instabilities of the alongshore current (which have a small pressure signature) contribute significantly to the infragravity velocity field. Based on the linear stability analysis of Bowen and Holman (1989), shear waves are expected to develop in the region of seaward shear in $\overline{V}$ and thus migrate onshore and offshore in a similar fashion as the $\overline{V}$ profile.

Later in the experiment, the Delilah bathymetry exhibits a well-developed bar–trough sequence (Figs. 2 and 3). These bathymetric changes are caused by large swell observed on 12 October during the passage of Hurricane Lily (note the sudden depth increase in Fig. 4). However, the tidal modulation of the mean alongshore current and infragravity velocities does not persist during this event. Thornton and Kim (1993) show that the cross-shore profile of the mean alongshore current is relatively stationary during this high wave event.

The relative contributions of shear and gravity waves to the infragravity band are examined with $R$, the normalized velocity to pressure variance ratio (16). The observed evolution of $R$ at each sensor position (2–9) is shown in Fig. 5 for the duration of the experiment. Estimates from sensor 1 are not shown because the current meter was submerged only at high tides. During the early part of the experiment, the current meter at position 2 (approximately 25 m offshore) was also exposed at lower stands of the tide (thus the measured velocities go to zero) and the ratios approach zero at those times.

Well offshore of the bar crest (sensors 8–9), the observed $R$ are close to the theoretical value for gravity waves ($R = 1$), suggesting that shear wave contributions are small. This is not surprising as the longshore current and associated shear waves are confined to the surf zone shoreward of these instruments. Only during the high energy conditions of 13 October do $R$ values >1 extend across the entire transect, consistent with a wide surf zone.

Observed values of $R$ inside the surf zone are often much greater than 1 (as high as 4), suggesting that shear waves contribute as much as 75% [Eq. (17)] of the total infragravity velocity variance at particular sensor positions. The tidal fluctuations in $R$ observed early in the experiment are generally in phase with the tide at the shallower stations (e.g., 2–3, Fig. 2) and 180 deg out of phase with the tide at deeper stations (e.g., 5–7). This is consistent with the on–offshore migration of shear waves that are confined to the seaward shear region of the longshore current profile. As this region moves onshore at high tide, shear wave variances (and $R$) increase at the inshore stations and decrease at the offshore stations (the opposite pattern occurs at low tide).

The cross-shore extent of the instabilities relative to the mean longshore current profile $\overline{V}(x)$ is illustrated in Figs. 6–8 with estimates of $R$ as a function of cross-shore position. Between 6 and 8 October when the bathymetry was terracelike and $\overline{V}$ strongly tidally modulated, the observed $R$ at low tides are close to the gravity wave value of 1 both outside the surf zone and shoreward of the maximum $\overline{V}$. In the region of strong seaward current shear the observed ratios are much higher ($R > 2$), indicating that shear waves contribute more than 50% [Eq. (17)] of the total infragravity velocity variance. Similar cross-shore variations in $R$ were observed from 14 to 16 October when the infragravity velocity variances and mean currents do not show a strong tidal variation (Fig. 7). Although the bottom profile has changed significantly to a well-developed bar–trough configuration, the observed $R > 1$ values indicative of shear waves are still confined to the region of seaward current shear. These results suggest that the region of energetic shear waves is controlled by the alongshore current distribution and insensitive to the bottom configuration, consistent with numerical results of Dodd and Thornton (1990).

The observations presented in Figs. 6–7 were obtained when the wave field was dominated by long-crested swell (periods 8–12 s) from the south. On 16 October when short-crested seas (periods 3–8 s) arrived from the north, similar cross-shore variations of $R$ are observed (Fig. 8), indicating predominantly shear waves ($R \approx 4$) in a narrow region of strong seaward shear in $\overline{V}$ and predominantly gravity waves ($R \approx 1$) where $\overline{V}$ is small.

## 6. Discussion

The spatial distribution of shear wave energy predicted by linear stability analysis (Bowen and Holman 1989) depends on the gradient of the background vorticity field $(\partial\overline{V}/\partial x)h^{-1}$. Numerical calculations (Dodd and Thornton 1990; Dodd et al. 1992; Putrevu and Svendsen 1992) show that the shear wave energy distribution is controlled primarily by the alongshore current profile rather than the depth profile, a result consistent with the observed similar cross-shore extent and synchronous tidal modulations (i.e., on–offshore migration) of $R$ and $\overline{V}$ profiles.

As instabilities grow in magnitude, an associated cross-shore mixing of momentum may cause a broadening of the alongshore current (Bowen and Holman 1989; Dodd and Thornton 1990; Putrevu and Svendsen 1992). Recent nonlinear theoretical and numerical analyses by Allen et al. (1996) suggest that instabilities eventually break up in strong eddies that migrate both shoreward into the trough of the sandbar and seaward well outside the surf zone, and thus can mix momentum across and beyond the surf zone. The predicted strength of the nonlinear instabilities depends not only on the alongshore current distribution but on friction coefficients, which are poorly understood. The wavenumber–frequency spectrum of the nonlinear instabilities was indistinguishable from the linear results, suggesting that wavenumber analysis may not resolve the nature of the shear waves. Still, if the nonlinear instabilities were indeed present in the velocity field during the Delilah experiment, then velocity to pressure variance ratios would be expected to be greater than the gravity wave prediction both seaward and shoreward of the region of seaward shear in the mean current. Although the present analysis does not preclude the breakdown of shear waves in eddies, the contributions of these eddies to the observed infragravity motions outside the surf zone appears to be small. Numerical calculations, such as those presented by Allen et al. (1996), and more extensive array observations are needed to characterize the evolution of shear waves in field data.

The observations suggest that shear waves are confined to a sometimes very narrow region of strong seaward shear in the alongshore current. Since the beach and alongshore current profiles may vary considerably over the course of an experiment, it is difficult to determine where to deploy an alongshore array of instruments to best measure the alongshore wavenumber spectrum of shear waves. During Delilah there were two alongshore arrays: a six-element array of bidirectional current meters located approximately in the trough of the sandbar (cross-shore position of sensor 3, Fig. 2) and a five-element array located on the seaward flank of the bar (cross-shore position of sensor 7). Although these arrays were capable of resolving the alongshore mode mix of edge and leaky waves, they were not always in the most advantageous position to detect shear waves. At times strong shear wave activity was confined entirely to a narrow region between the alongshore arrays (e.g., Fig. 6).

## 7. Conclusions

The cross-shore variability of infragravity-frequency (0.004–0.05 Hz) motions on a naturally barred beach is examined with field measurements from a cross-shore array of collocated pressure sensors and bidirectional current meters. Infragravity pressure and velocity variances are compared at nine positions spanning the width of the surf zone from very near the beach face to 4.5-m depth. Ratios of velocity to pressure variances are used to make qualitative assessments of the relative contributions by shear waves (instabilities of the longshore current) and gravity (edge and leaky) waves.

Simple analytical expressions for velocity (both cross-shore, $u$, and alongshore, $v$, components) and pressure ($p$) variances are derived for edge waves on a plane beach under the assumption that the energy for low mode numbers is distributed uniformly over a wide wavenumber range. Predicted $p$ variances decay seaward as $h^{-1}$. Predicted $u$ and $v$ variances are equal and decay seaward as $h^{-2}$. These depth dependencies and isotropic velocities are consistent with a WKB approximation for a broad spectrum of trapped waves (Herbers et al. 1995a). In contrast, close to shore, leaky waves (and high-mode edge waves) have $p$ and $u$ ($v \approx 0$) variances decay proportional to $h^{-1/2}$ and $h^{-3/2}$, respectively. The total velocity ($u$ and $v$) to pressure variance ratio is $g/h$ for gravity waves, independent of the edge–leaky wave mode mix. Numerical calculations of velocity to pressure variance ratios in broad edge wave spectra on barred beach profiles do not deviate significantly from the plane beach predictions (less than about 15% for typical profiles of natural beaches). In shear waves, surface excursions are small (Bowen and Holman 1989), and velocity to pressure variance ratios are much larger than the gravity wave value $g/h$. Thus, observed velocity to pressure variance ratios can be used to estimate the contributions of gravity and shear waves to the infragravity band.

Estimates of velocity to pressure variance ratios indicate that shear waves contribute significantly (as much as 75%) to the total infragravity velocity variance in the region of strong seaward shear of the alongshore current profile. Both shoreward and seaward of this region the observed ratios are approximately equal to the gravity wave value $g/h$, indicating an infragravity spectrum composed primarily of gravity (edge and/or leaky) waves. Strong shear wave activity is consistently observed in the region of strong shear in the alongshore current, independent of large changes in the beach profile. This result is qualitatively consistent with numerical results of Dodd and Thornton (1990).

*Acknowledgments*

This work was sponsored by the Office of Naval Research, Coastal Dynamics Program. Logistical support for Delilah

was provided by the staff of the U.S. Army Field Research Facility, Duck, North Carolina, led by Bill Birkemeier. Tim Stanton and Rob Wyland of the Naval Postgraduate School designed, built, and maintained the data acquisition system for Delilah. The numerical calculations were performed with computer code generously provided by Peter Howd. Jurjen Battjes pointed out the similarity of our edge wave results with the equal partitioning of potential and kinetic energy in progressive gravity waves. This work also benefited from several insightful discussions with John Allen and from the helpful comments of the anonymous reviewers.

---

## REFERENCES

Allen, J. S., P. A. Newberger, and R. A. Holman, 1996: Nonlinear shear instabilities of alongshore currents on plane beaches. *J. Fluid Mech.,* **310,** 181–213..

Birkemeier, W. A., 1991: Delilah nearshore processes experiment: Data summary, miscellaneous reports. Coastal Eng. Res. Cent., Field Res. Facil., U.S. Army Eng. Waterw. Exp. Sta., Vicksburg, Miss..

Bowen, A. J., and R. T. Guza, 1978: Edge waves and surf beat. *J. Geophys. Res.,* **83,** 1913–1920..

— ,and R. A. Holman, 1989: Shear instabilities of the mean longshore current 1. Theory. *J. Geophys. Res.,* **94,** 18 023–18 030..

Dodd, N., and E. B. Thornton, 1990: Growth and energetics of shear waves in the nearshore. *J. Geophys. Res.,* **95,** 16 075–16 083..

— ,J. M. Oltman-Shay, and E. B. Thornton, 1992: Shear instabilities in the longshore current: A comparison of observation and theory. *J. Phys. Oceanogr.,* **22,** 62–82.. Find this article online

Eckart, C., 1951: Surface waves on water of variable depth. Wave Rep. 100, Scripps Institution of Oceanography, University of California, San Diego, La Jolla, CA, 99 pp..

Guza, R. T., and E. B. Thornton, 1985: Observations of surf beat. *J. Geophys. Res.,* **90,** 3161–3172..

Herbers, T. H. C., S. Elgar, R. T. Guza, and W. C. O'Reilly, 1995a: Infragravity-frequency (0.005–0.05 Hz) motions on the shelf. Part II: Free waves. *J. Phys. Oceanogr.,* **25,** 1063–1079.. Find this article online

— ,— ,and — ,1995b: Generation and propagation of infragravity waves. *J. Geophys. Res.,* **100,** 24 863–24 872..

Holman, R. A., 1981: Infragravity energy in the surf zone. *J. Geophys. Res.,* **86,** 6442–6450..

— ,and A. J. Bowen, 1979: Edge waves on complex bathymetry. *J. Geophys. Res.,* **84,** 6339–6346..

— ,and A. H. Sallenger, 1985: Setup and swash on a natural beach. *J. Geophys. Res.,* **90,** 945–953..

Howd, P. A., J. M. Oltman-Shay, and R. A. Holman, 1991: Wave variance partitioning in the trough of a barred beach. *J. Geophys. Res.,* **96,** 12 781–12 795..

— ,A. J. Bowen, and R. A. Holman, 1992: Edge waves in the presence of strong longshore currents. *J. Geophys. Res.,* **97,** 11 357–11 371..

Huntley, D. A., 1976: Long period waves on a natural beach. *J. Geophys. Res.,* **81,** 6441–6449..

— ,R. T. Guza, and E. B. Thornton, 1981: Field observations of surf beats. 1. Progressive edge waves. *J. Geophys. Res.,* **86,** 6451–6466..

Kenyon, K. E., 1972: Edge waves with current shear. *J. Geophys. Res.,* **77,** 6599–6603..

Kirby, J. T., R. A. Dalrymple, and P. L.-F. Liu, 1981: Modification of edge waves by barred beach topography. *Coastal Eng.,* **5,** 35–49..

Munk, W. H., 1949: Surf beats. *Eos, Trans. Amer. Geophys. Union,* **30,** 849–854..

Oltman-Shay, J. M., and R. T. Guza, 1987: Infragravity edge wave observations on two California beaches. *J. Phys. Oceanogr.,* **17,** 644–663.. Find this article online

— ,P. A. Howd, and W. A. Birkemeier, 1989: Shear instabilities of the mean longshore current 2. Field observations. *J. Geophys. Res.,* **94,** 18 031–18 042..

Putrevu, U., and I. A. Svendsen, 1992: Shear instability of longshore currents: A numerical study. *J. Geophys. Res.*, **97,** 7283–7303..

Sallenger, A. H., and R. A. Holman, 1987: Infragravity waves over a natural barred profile. *J. Geophys. Res.*, **92,** 9531–9540..

Suhayda, J. N., 1974: Standing waves on beaches. *J. Geophys. Res.*, **79,** 3065–3071..

Thornton, E. B., and R. T. Guza, 1982: Energy saturation and phase speeds measured on a natural beach. *J. Geophys Res.*, **87,** 9499–9508..

— ~~,~~ and C. S. Kim, 1993: Longshore current and wave height modulation at tidal frequency inside the surf zone. *J. Geophys. Res.*, **98,** 16 509–16 519..

---

## Figures

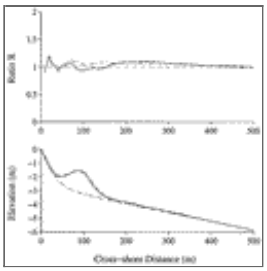

Click on thumbnail for full-sized image.

Fig. 1. Example numerical results showing the effect of nonplanar topography on the normalized velocity to pressure variance ratio *R* of edge waves. Results for synthetic barred (dashed line) and concave (dashed–dot line) beach profiles are compared to the theoretical value 1 for a plane beach. The actual measured profile (solid line) from 11 October is also shown in the lower panel.

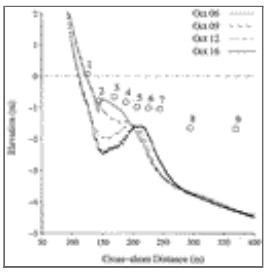

Click on thumbnail for full-sized image.

Fig. 2. Depth profiles for four days during the Delilah experiment (from Thornton and Kim 1993). The symbols indicate the horizontal and vertical positions of the current meters and pressure sensors.

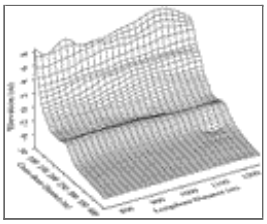

Click on thumbnail for full-sized image.

Fig. 3. An example bathymetry map from 12 October. The morphology is characterized by an approximately linear bar feature 80 m offshore. The instrumented transect is at longshore position 986 m.

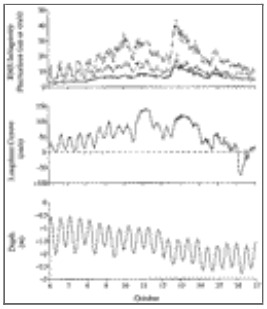

Click on thumbnail for full-sized image.

Fig. 4. Evolution of root-mean-square infragravity pressure (solid line) and velocity (cross-shore component: dashed–dot line; longshore component: dashed line) fluctuations (upper panel) observed at sensor 4 located approximately 70 m offshore (see Fig. 2). Also shown is the mean longshore velocity at that location (center panel), and the water depth (lower panel).

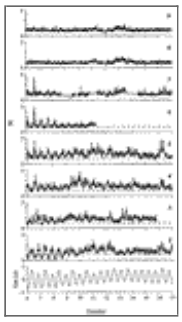

Click on thumbnail for full-sized image.

Fig. 5. Evolution of observed normalized velocity to pressure variance ratios $R$ for sensors 2–9 (sensor 1 is not shown as it is submerged only at high tides). The cross-shore location of the sensor is indicated in Fig. 2, and the tide elevation is shown in the bottom panel. The theoretical ratio for gravity (edge and leaky) waves ($R = 1$) is indicated with a dashed line in each panel.

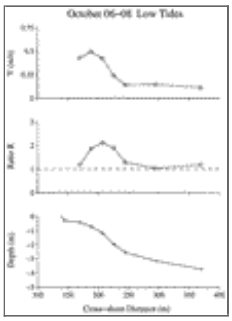

Click on thumbnail for full-sized image.

Fig. 6. The observed ratio $R$ as a function of cross-shore distance (center panel) averaged over all low-tide observations during 6–8 October. Also shown is the average mean longshore current distribution (upper panel) and beach profile (lower panel).

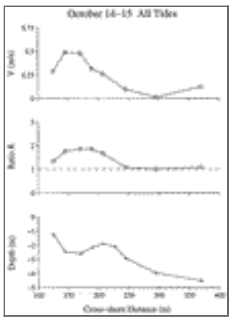

Click on thumbnail for full-sized image.

Fig. 7. Same as Fig. 6 but for 14–15 October including data at all tide stages.

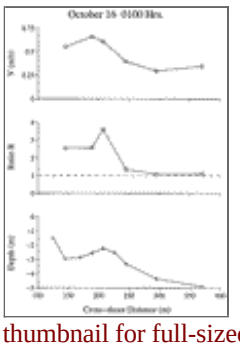

Click on thumbnail for full-sized image.

Fig. 8. Same as Fig. 6 but for a 2-h record on 16 October.

*Corresponding author address:* Dr. Thomas C. Lippman, Center for Coastal Studies, 0209, Scripps Institution of Oceanography, University of California, San Diego, 9500 Gilman Drive, La Jolla, CA 92093-0209.

E-mail: lippman@coast.ucsd.edu

top